Anti-apoE immunotherapy inhibits amyloid accumulation in a transgenic mouse model of Aβ amyloidosis

Jungsu Kim,[1,2,3] Adam E.M. Eltorai,[1,2,3] Hong Jiang,[1,2,3] Fan Liao,[1,2,3] Philip B. Verghese,[1,2,3] Jaekwang Kim,[1,2,3] Floy R. Stewart,[1,2,3] Jacob M. Basak,[1,2,3] and David M. Holtzman[1,2,3]

[1]Department of Neurology, [2]Hope Center for Neurological Disorders, and the [3]Knight Alzheimer's Disease Research Center, Washington University School of Medicine, Saint Louis, MO 63110

The apolipoprotein E (*APOE*) ε4 allele is the strongest genetic risk factor for Alzheimer's disease (AD). The influence of apoE on amyloid β (Aβ) accumulation may be the major mechanism by which apoE affects AD. ApoE interacts with Aβ and facilitates Aβ fibrillogenesis in vitro. In addition, apoE is one of the protein components in plaques. We hypothesized that certain anti-apoE antibodies, similar to certain anti-Aβ antibodies, may have antiamyloidogenic effects by binding to apoE in the plaques and activating microglia-mediated amyloid clearance. To test this hypothesis, we developed several monoclonal anti-apoE antibodies. Among them, we administered HJ6.3 antibody intraperitoneally to 4-mo-old male APPswe/PS1ΔE9 mice weekly for 14 wk. HJ6.3 dramatically decreased amyloid deposition by 60–80% and significantly reduced insoluble Aβ40 and Aβ42 levels. Short-term treatment with HJ6.3 resulted in strong changes in microglial responses around Aβ plaques. Collectively, these results suggest that anti-apoE immunization may represent a novel AD therapeutic strategy and that other proteins involved in Aβ binding and aggregation might also be a target for immunotherapy. Our data also have important broader implications for other amyloidosis. Immunotherapy to proteins tightly associated with misfolded proteins might open up a new treatment option for many protein misfolding diseases.

CORRESPONDENCE
David M. Holtzman:
holtzman@neuro.wustl.edu

Abbreviations used: Aβ, amyloid β; AD, Alzheimer's disease; APOE, apolipoprotein E; APP, Aβ precursor protein; PS, presenilin; RIPA, radioimmunoprecipitation assay.

Accumulation of amyloid β (Aβ) peptide in the brain is hypothesized to initiate pathogenic cascades that lead to Alzheimer's disease (AD; Golde et al., 2011; Holtzman et al., 2011). Therapeutic strategies to inhibit Aβ accumulation, such as Aβ immunotherapy, are currently being tested as disease-modifying therapies (Golde et al., 2011; Holtzman et al., 2011). Sequential proteolytic cleavages of Aβ precursor protein (APP) by β- and γ-secretase produce the Aβ peptide. Although rare, early-onset AD mutations in the *APP*, *presenilin 1* (*PS1*), and *PS2* genes have supported the critical role of Aβ in AD pathogenesis, the ε4 allele of *apolipoprotein E* (*APOE*) gene is the strongest genetic risk factor for the common late-onset form of AD, and the ε2 allele is protective (Kim et al., 2009a). Among several mechanisms proposed to explain the effects of apoE on AD pathogenesis, prevailing evidence suggests that apoE's effect on Aβ accumulation may be the major mechanism (Kim et al., 2009a). ApoE appears to affect Aβ accumulation by modulating both Aβ aggregation and clearance (Ma et al., 1994; Wisniewski et al., 1994; Castano et al., 1995; Sadowski et al., 2006; Deane et al., 2008; Jiang et al., 2008; Castellano et al., 2011). Along with other amyloid-associated proteins, apoE is found in amyloid plaques (Namba et al., 1991; Wisniewski and Frangione, 1992). In this study, we hypothesized that after peripheral administration of monoclonal anti-apoE antibodies, the small fraction of anti-apoE antibodies that enter the brain would bind to apoE in plaques and decrease Aβ accumulation by activating microglia-mediated clearance of Aβ aggregates, similar to what has been described for certain anti-Aβ antibodies (Bard et al., 2000; Brody and Holtzman, 2008).

The Rockefeller University Press $30.00
J. Exp. Med. 2012 Vol. 209 No. 12 2149-2156
www.jem.org/cgi/doi/10.1084/jem.20121274

The Journal of Experimental Medicine

RESULTS AND DISCUSSION

Generation and characterization of anti-apoE antibodies

To characterize anti-apoE antibodies, we evaluated their performance in Western blotting, ELISA, immunohistochemistry, and immunoprecipitation. For Western blotting application, cortical tissues from wild-type C57BL6/CBA background mice were lysed with radioimmunoprecipitation assay (RIPA) buffer and used for detection of apoE protein. Cortical tissue lysates from *apoe* KO mice were used as negative controls. Among four HJ antibodies tested, HJ6.3 antibody (IgG2b isotype) gave the strongest signal in Western blotting (Fig. 1 A). When the membranes were overexposed, other antibodies also recognized apoE (Fig. 1 B). For sandwich ELISA application, anti-apoE antibody (WUE4) was used as a capture antibody, and then a different concentration of lipid-free apoE protein (0, 0.25, 0.74, 2.22, 6.67, 20, 60, and 180 ng/ml) was added to

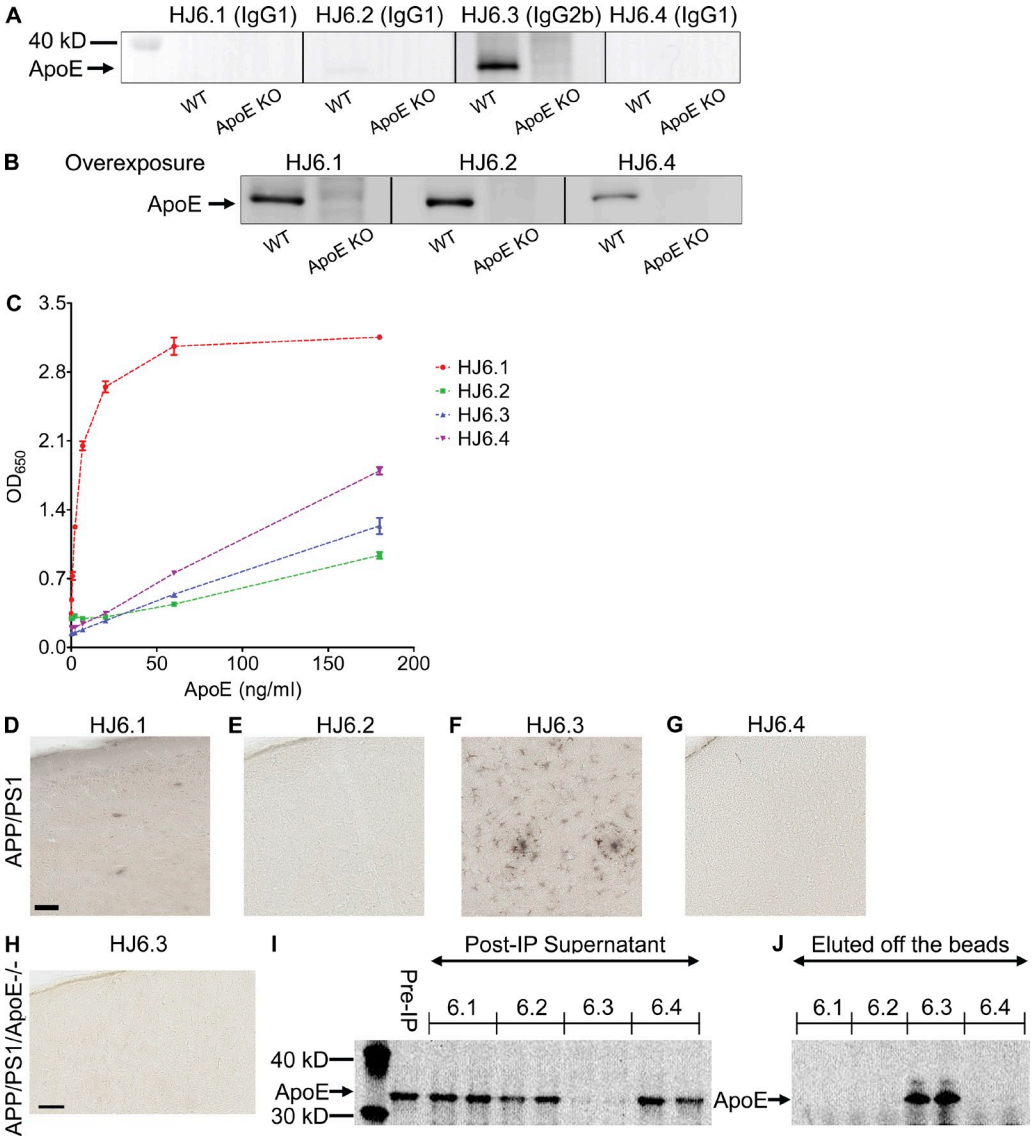

Figure 1. Characterization of anti-apoE antibodies. Four different anti-apoE antibodies were tested for their ability to recognize apoE in Western blotting (A and B), ELISA (C), immunohistochemistry (D–H), and immunoprecipitation (I). (A and B) Cerebral cortical tissues from wild-type and *apoe* KO mice were lysed with RIPA buffer and equal amounts of total proteins were loaded to each well. In B, the membranes shown in A were overexposed to show a weak apoE band in the membranes probed with HJ6.1, HJ6.2, and HJ6.4 antibody. (C) ELISA plates were coated with anti-apoE antibody (WUE4), and each biotinylated HJ antibody was used as a detection antibody. Optical density at 650 nm was measured with a series of different *apoe* concentrations. (D–G) Biotinylated HJ antibody was used as a primary antibody in the immunohistochemical staining with APPswe/PS1ΔE9 mice brain tissues. Bar, 50 µm. (H) Biotinylated HJ6.3 antibody was used as a primary antibody in the immunohistochemical staining with brain tissues from apoE-deficient APPswe/PS1ΔE9 mice. Bar, 50 µm. (I and J) Cerebral cortical tissues from wild-type mice were lysed with RIPA buffer, and the RIPA lysates were used for immunoprecipitation with each HJ antibody. ApoE proteins left in the supernatant of postimmunoprecipitation (Post-IP) solution (I) and eluted from protein G–Sepharose beads (J) were detected with a polyclonal anti-apoE antibody (EMD Millipore).

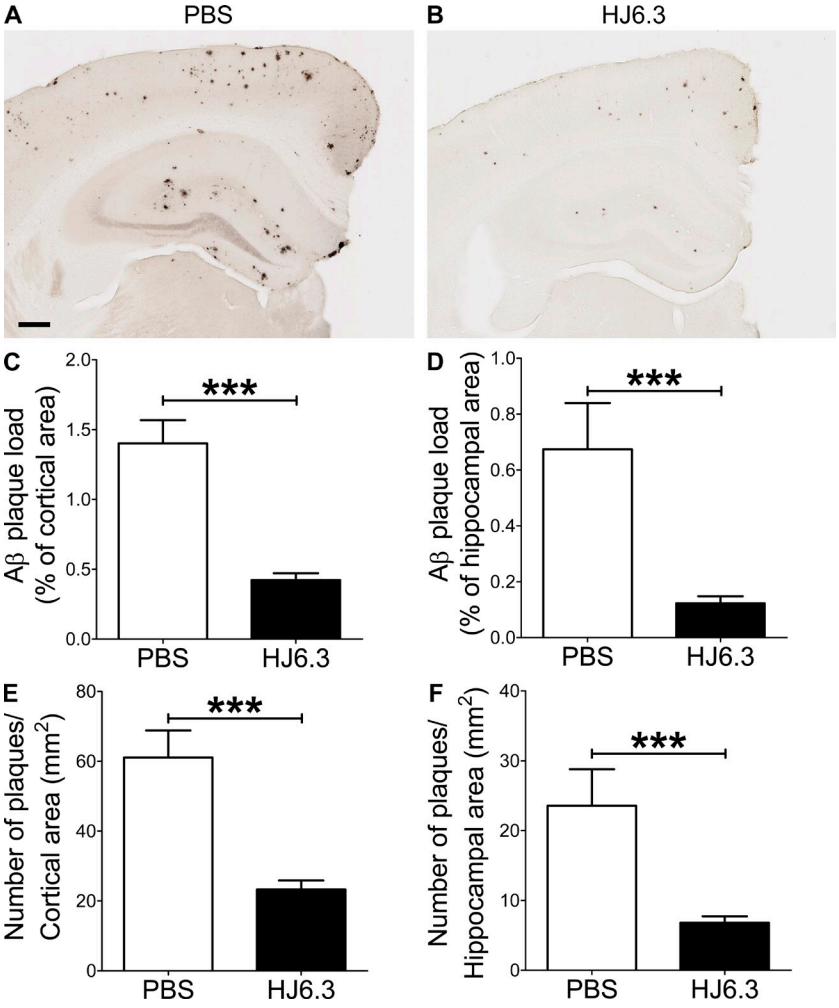

Figure 2. Reduction of Aβ plaque depositions by anti-apoE immunotherapy. 4-mo-old male APPswe/PS1ΔE9 mice were intraperitoneally injected with PBS vehicle or anti-apoE antibody (HJ6.3) weekly for 14 wk. (A and B) Brain sections from 7-mo-old mice were immunostained for Aβ plaques with anti-Aβ antibody (82E1-biotin). Bar, 250 µm. The extent of Aβ plaque load was quantified in cortex (C) and hippocampus (D). The number of plaques per unit area was quantified in cortex (E) and hippocampus (F). $n = 7$ for PBS group; $n = 18$ for HJ6.3 group. To determine the statistical significance (***, $P < 0.001$), a two-tailed Student's t test was used. Variance in all graphs represents SEM.

each well in the ELISA plates. Each biotinylated HJ antibody was used as a detection antibody in the sandwich ELISA format (Fig. 1 C). Although all HJ6 antibodies recognized apoE in the ELISA, HJ6.1 antibody (IgG1 isotype) generated the strongest signals. Although HJ6 antibodies were initially screened based on their recognition of purified, astrocyte-secreted, lipidated apoE lipoprotein particles, all of them also recognized lipid-free apoE (Fig. 1, A–C).

To determine whether HJ antibodies can detect apoE in amyloid plaques in the brain, we stained brain tissue sections from amyloid plaque–bearing 7-mo-old APPswe/PS1ΔE9 mice (Jankowsky et al., 2004; Fig. 1, D–G). HJ6.3 antibody was the only antibody that recognized apoE associated with amyloid plaques and in astrocytes, which are the major producers of apoE in the brain (Kim et al., 2009a; Fig. 1 F). To evaluate the specificity of HJ6.3 antibody to apoE, we used cortical tissues from APPswe/PS1ΔE9 mice that lacked the *apoe* gene (APP/PS1/*apoe*$^{-/-}$ mice) as negative controls. When HJ6.3 antibody was used as a primary antibody in the immunohistochemical staining, it did not give any detectable signal with the tissues from APP/PS1/*apoe*$^{-/-}$ mice, thereby validating the specificity of HJ6.3 antibody to apoE in tissue sections (Fig. 1 H). For immunoprecipitation application, each HJ antibody was first covalently conjugated to Sepharose beads and then incubated with 1% Triton X-100 cortical tissue lysates. The supernatants from immunoprecipitation (Fig. 1 I) and the eluents from the Sepharose beads (Fig. 1 J) were used in Western blotting to assess efficiency of immunoprecipitation. Levels of apoE were measured using a polyclonal anti-apoE antibody (EMD Millipore) by Western blotting. HJ6.3 antibody was the only antibody that was able to bind to apoE in cortical tissue lysates, resulting in successful immunoprecipitation.

Anti-apoE immunotherapy inhibits amyloid accumulation in the brain

Given its ability to detect apoE in amyloid plaques (Fig. 1 F), we selected HJ6.3 antibody for anti-apoE immunization experiments. To determine whether anti-apoE antibody would have an antiamyloidogenic effect, we injected PBS or anti-apoE antibody (HJ6.3) weekly at 10 mg of antibody/kg of body weight per dose. 4-mo-old male APPswe/PS1ΔE9 mice were intraperitoneally injected for 14 wk. Brain tissues were processed for histochemical and biochemical analyses. Quantitative analyses of anti-Aβ immunostaining (Fig. 2, A and B)

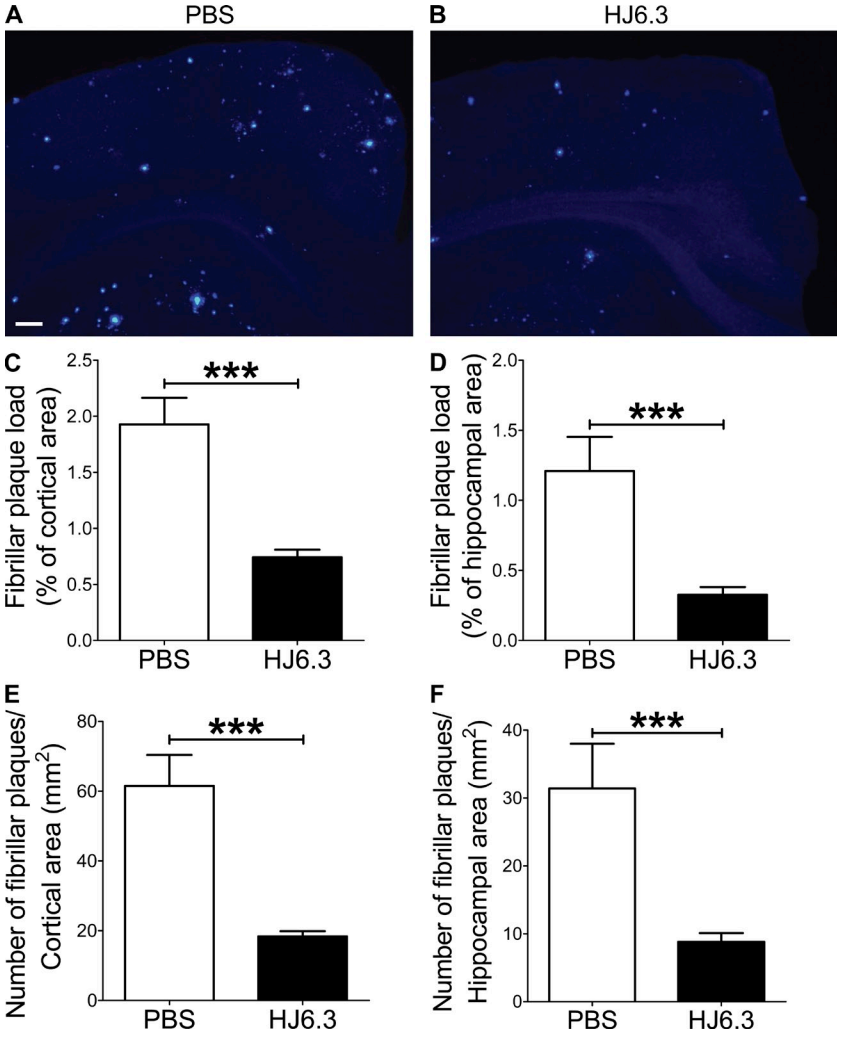

Figure 3. Attenuation of fibrillar amyloid accumulations by anti-apoE immunotherapy. (A and B) Brain sections from male mice injected with PBS or HJ6.3 antibody were stained with X-34 dye that recognizes only fibrillar plaques with a β-sheet conformation. Bar, 150 µm. The extent of fibrillar plaque load was quantified from cortex (C) and hippocampus (D). The number of fibrillar plaques per unit area was quantified from cortex (E) and hippocampus (F). $n = 7$ for PBS group; $n = 18$ for HJ6.3 group. Variance in all graphs represents SEM.

demonstrated that Aβ plaque load in the cortex (Fig. 2 C) and hippocampus (Fig. 2 D) was markedly decreased by HJ6.3 antibody treatment, compared with the PBS-treated control group. There was a strong 70–80% reduction in Aβ plaque load in the cortex (Fig. 2 C) and hippocampus (Fig. 2 D). HJ6.3 treatment also significantly decreased the number of plaques per area in the cortex (Fig. 2 E) and hippocampus (Fig. 2 F). To further characterize the structural nature of the deposited Aβ plaques, brain sections were stained with X-34 dye that selectively recognizes only fibrillar Aβ deposits (Fig. 3, A and B). Consistent with the anti-Aβ antibody staining results (Fig. 2), the HJ6.3-treated group had significantly less X-34–positive fibrillar plaque load (Fig. 3, C and D) and a decrease in the number of fibrillar plaques per area (Fig. 3, E and F) in the cortex (Fig. 3, C and E) and hippocampus (Fig. 3, D and F). To determine the effect of HJ6.3 antibody on insoluble Aβ accumulation, we performed Aβ end-specific ELISA. Cortical and hippocampal tissues were sequentially homogenized with PBS and 5 M guanidine HCl buffer. Significant reductions in insoluble Aβ40 (Fig. 4, A and C) and Aβ42 (Fig. 4, B and D) levels were observed in the cortex (Fig. 4, A and B) and hippocampus (Fig. 4, C and D) of mice treated with HJ6.3 antibody. Collectively, our results clearly demonstrate that anti-apoE antibody HJ6.3 treatment dramatically inhibits Aβ aggregation and amyloid accumulation in the brain.

Anti-apoE antibody treatment does not affect levels of cholesterol and apoE

ApoE lipoprotein plays a key role in the receptor-mediated endocytosis of lipoprotein particles in the plasma, thereby regulating plasma cholesterol levels (Kim et al., 2009a). It is conceivable that long-term treatment of anti-apoE antibody may alter plasma cholesterol metabolism by interfering with a normal function of apoE in the periphery. To assess this potential concern, we measured total cholesterol levels in the plasma from the APP/PS1 mice treated for 14 wk. No significant difference in total cholesterol levels was observed between the PBS-treated and HJ6.3 antibody-treated groups (PBS group, 151.0 ± 13.82 mg/dl; HJ6.3 group, 140.0 ± 12.45 mg/dl; P = 0.598; 95% confidence interval,

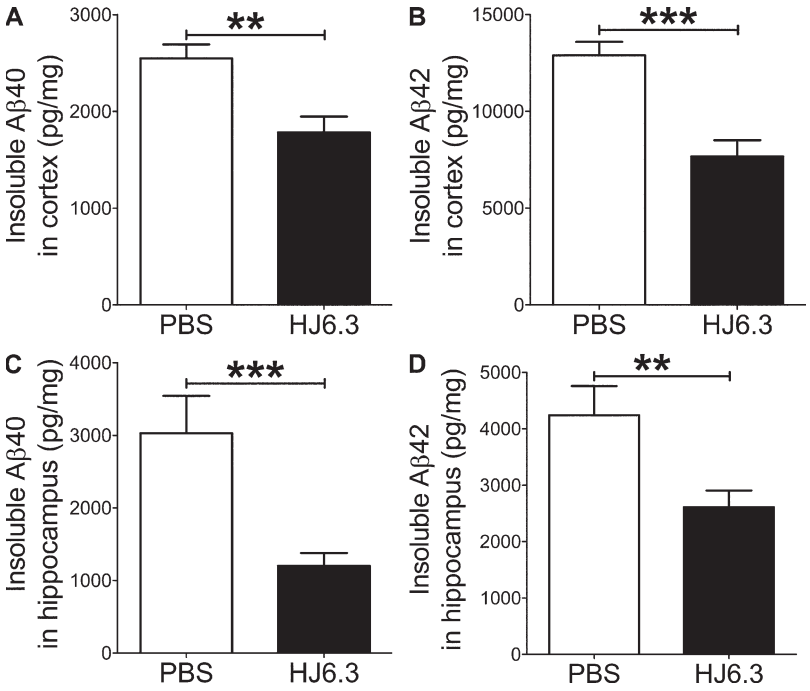

Figure 4. Decrease of insoluble Aβ levels by anti-apoE immunotherapy. Cortical and hippocampal tissues from male mice injected with PBS or HJ6.3 antibody were first homogenized with PBS. Aggregated forms of Aβ in the PBS-insoluble pellet were solubilized with 5M guanidine HCl buffer. Insoluble Aβ40 (A) and Aβ42 (B) levels in cortex were measured using an Aβ-end specific ELISA. Similarly, insoluble Aβ40 (C) and Aβ42 (D) levels in hippocampus were measured using Aβ end-specific ELISA. $n = 7$ for PBS group; $n = 18$ for HJ6.3 group. Variance in all graphs represents SEM.

−34.16–56.23). In addition, there was no significant change in apoE levels between two groups (cortex apoE in PBS group, 6.026 ± 0.1783 ng/mg of wet brain weight; cortex apoE in HJ6.3 group, 6.507 ± 0.3107 ng/mg of wet brain weight; P = 0.25; 95% confidence interval, −1.340–0.3773; plasma apoE in PBS group, 207.1 ± 25.01 μg/ml; plasma apoE in HJ6.3 group, 192.3 ± 13.54 μg/ml; P = 0.58; 95% confidence interval: −39.21–68.90). Body weights of both groups were similar (PBS group, 45.57 ± 0.8226 g; HJ6.3 group, 45.26 ± 1.154 g; P = 0.8340; 95% confidence interval: −2.691–3.314). Collectively, these data indicate that anti-apoE immunotherapy with HJ6.3, when given weekly, does not influence brain apoE, peripheral cholesterol metabolism, and general health.

Anti-apoE antibody treatment recruits microglia around plaques and decreases levels of proinflammatory cytokines

Several mechanisms have been proposed to explain the beneficial effects of anti-Aβ immunotherapy (Brody and Holtzman, 2008; Golde et al., 2009). Among them, recruitment and activation of microglia triggered by antibody in the brain appears to be one of main underlying mechanisms (Koenigsknecht-Talboo et al., 2008; Wang et al., 2011). The level of HJ6.3 antibody detected in the brain 24 h after a single injection was 0.096 ± 0.019% of the level present in the plasma. To determine whether HJ6.3 antibody can increase the amount of microglia around plaques, we quantified $CD45^+$ microglia after short-term treatment of HJ6.3 antibody (intraperitoneal injection 4 times every 3 d) in mice that already had existing plaques at 9 mo of age. Brain tissues were collected 1 d after the fourth injection. To quantitatively assess the extent of microglial activation, we used an anti-CD45 antibody that recognizes activated microglia around plaques (Fig. 5, A and B). Previous studies demonstrated that fibrillar amyloid plaques are strongly associated with the activation of microglia (Lucin and Wyss-Coray, 2009). Because we used 9-mo-old APPswe/PS1ΔE9 mice with preexisting fibrillar plaques (Jankowsky et al., 2004), we calculated HJ6.3-induced microglial activation after normalizing with fibrillar plaque load. Fibrillar plaque load was measured from subsequent adjacent sections (50 μm apart) stained with the fibrillar amyloid–detecting dye X-34. Quantitative analyses indicted that anti-apoE antibody HJ6.3 significantly increased CD-45 staining associated with amyloid plaques (Fig. 5 C), suggesting HJ6.3-mediated recruitment of microglia around plaques.

To better characterize the type of inflammatory response mediated by HJ6.3 antibody, we measured levels of several cytokines in cortical tissue lysates. Using Rodent Cytokine MAP kit (Myriad RBM), we measured the levels of IFN-γ, IL-1α, IL-1 β, IL-4, IL-6, IL-10, IL-12p70, and tumor necrosis factor α. Although most cytokines in the cortex were below detection limit, levels of IFN-γ, IL-1α, and IL-10 were reliably measured. Although the levels of proinflammatory cytokines (IFN-γ and IL-1α) were significantly decreased by anti-apoE antibody treatment (Fig. 5, D and E), the antiinflammatory cytokine IL-10 showed a trend toward increased level (PBS group, 10.88 ± 1.061 pg/mg of total protein; HJ6.3 group, 13.65 ± 1.855 pg/mg of total protein; P = 0.21). In the 14-wk long-term treatment experiments, HJ6.3 treatment did not cause any significant change in the cytokine levels (unpublished data). No effect on cytokine is likely caused by an extended time delay (10 d) between the last antibody injection and tissue collection in the long term treatment paradigm. Collectively, these data suggest that anti-apoE immunotherapy acutely modulates inflammatory response of microglia to amyloid plaques.

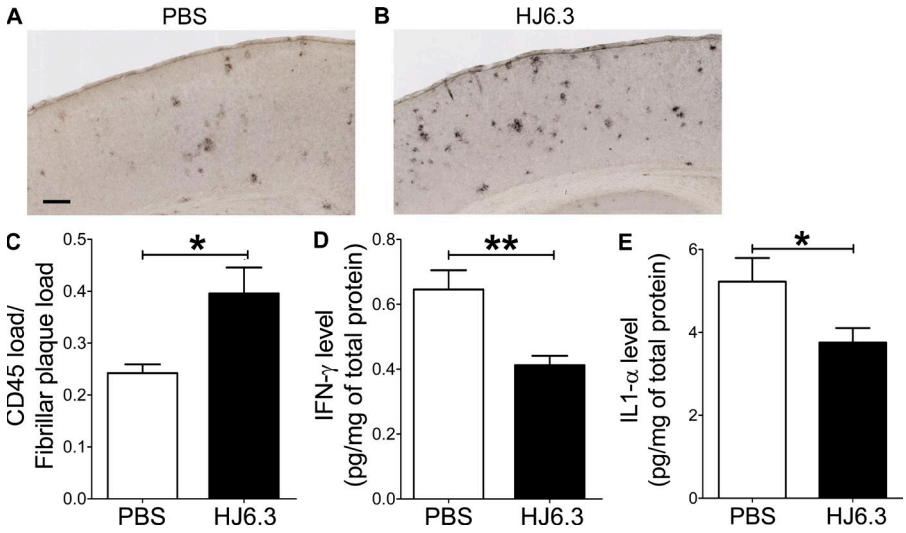

Figure 5. Modulation of microglia activity by anti-apoE antibody treatment. APPswe/PS1ΔE9 mice were intraperitoneally injected with PBS vehicle or anti-apoE antibody (HJ6.3; 10 mg/kg) 4 times every 3 d. (A and B) Brain sections were immunostained for activated microglia with anti-CD45 antibody. Bar, 150 µm. (C) The extent of microglial recruitment around plaques in cortex was quantified after normalizing with X-34–positive fibrillar plaque load. (D and E) Levels of proinflammatory cytokines (IFN-γ and IL-1α) in the cortex were measured by Rodent Cytokine Multi-Analyte Profile assay. $n = 11$ for PBS group; $n = 9$ for HJ6.3 group. Variance represents SEM.

In the current study, we hypothesized that anti-apoE antibodies may have anti-amyloidogenic effects, by binding to apoE in amyloid plaques and activating microglia-mediated Aβ clearance. Weekly intraperitoneal injection of anti-apoE antibody HJ6.3 over 14 wk dramatically reduced amyloid plaque deposition and insoluble Aβ accumulation in the cortex and hippocampus, without altering plasma cholesterol levels. These data suggest that anti-apoE immunization strategy may be further explored as a potential therapeutic strategy in AD. In addition, our finding may help further elucidate the precise function of apoE in AD pathogenesis. Previously, a variety of different anti-Aβ antibodies have been shown to inhibit Aβ accumulation in mouse models of Aβ amyloidosis, and they are considered promising disease-modifying therapies (Brody and Holtzman, 2008; Golde et al., 2009). However, passive immunotherapy targeting other components of Aβ plaques, such as apoE, has not been previously considered. We demonstrate that passive immunization against Aβ-associated protein, apoE, can be very effective in attenuating Aβ accumulation. Along with a recent study using active vaccination with ankyrin G (Santuccione et al., 2012), our finding opens up a new avenue of research to target other components in amyloid plaques, such as apoE, apolipoprotein J/clusterin, and heparin sulfate proteoglycans.

Recruitment and activation of microglia around plaques and subsequent Aβ degradation/clearance have been proposed as one of the mechanisms by which Aβ immunotherapy decreases amyloid levels (Bard et al., 2000; Koenigsknecht-Talboo et al., 2008; Wang et al., 2011). In our study, anti-apoE antibody HJ6.3 significantly increased CD45-positive microglia around amyloid plaques and decreased proinflammatory cytokines. This finding suggests that anti-apoE antibody might modulate similar inflammatory responses, which is consistent with the effect of certain anti-Aβ antibodies (Bard et al., 2000; Wilcock et al., 2004). Anti-apoE antibodies may recruit microglia to apoE-containing plaques, triggering both direct phagocytosis and the attenuation of proinflammatory cytokines, leading to reduction in amyloid accumulation.

Considering the direct effects of apoE on Aβ clearance and aggregation (Kim et al., 2009a), other mechanisms could theoretically be involved in anti-apoE antibody-mediated reduction in amyloid accumulation. Several studies demonstrated that apoE modulates Aβ clearance (Kim et al., 2009a). Binding of apoE to Aβ may slow down Aβ clearance in the brain, therefore increasing Aβ accumulation. This possibility is supported by the fact that mice lacking apoE have faster Aβ clearance, relative to apoE-expressing mice (DeMattos et al., 2004). Anti-apoE antibody may bind to soluble apoE, thereby attenuating apoE-mediated impairment of Aβ clearance. Another mechanism could be related with the direct influence of apoE on Aβ fibrillogenesis. Previous studies have demonstrated that apoE increases Aβ fibrillogenesis under certain in vitro Aβ aggregation conditions (Ma et al., 1994; Wisniewski et al., 1994; Castano et al., 1995). Anti-apoE antibody could physically interfere with the interaction between apoE and Aβ, thereby decreasing the fibrillogenic effect of apoE on Aβ. A similar strategy preventing the interaction between apoE and Aβ has already been successfully used to attenuate Aβ toxicity and amyloid deposition (Sadowski et al., 2006). Similar mechanisms may mediate antiamyloidogenic phenotypes observed in *apoe* haploinsufficient mouse models (Bien-Ly et al., 2012; Kim et al., 2011). In the current study, we administered anti-apoE antibody to 4-mo-old male APPswe/PS1ΔE9 mice when they had just started to develop amyloid deposition. Previous studies have demonstrated that anti-Aβ antibodies can effectively decrease amyloid accumulation when they are given preventatively, but they are less effective in a treatment mode (Brody and Holtzman, 2008; Golde et al., 2009). In future studies, it will be important to determine whether anti-apoE antibodies will prevent the detrimental effects of apoE and have therapeutic effects on pathology, even when the treatment begins after significant amyloid deposition occurred in the brain.

MATERIALS AND METHODS

Generation of antibodies. To generate monoclonal anti-apoE antibodies, we first isolated apoE lipoprotein particles from primary astrocytes cultured from C57BL6 mice (The Jackson Laboratory) using an apoE antibody (EMD Millipore) immunoaffinity column. Purified, astrocyte-secreted, lipidated apoE lipoprotein particles were injected with complete Freund's adjuvant into *apoe* KO mice (The Jackson Laboratory). For an initial screening of antibodies, supernatants from hybridoma cells (~2,000 wells) were added to 96-well plates coated with purified, astrocyte-secreted, lipidated apoE lipoprotein particles. Using anti–mouse IgG-horseradish peroxidase as a detection antibody, we initially identified 36 clones, and then subcloned them to find those that performed well in several biochemical and immunohistochemical assays. Antibody isotype was determined using a mouse monoclonal antibody isotyping kit (GE Healthcare).

Immunoblotting. Cerebral cortical tissues from wild-type and *apoe* KO mice were lysed with RIPA lysis buffer (1% NP-40, 1% sodium deoxycholate, 0.1% SDS, 25 mM Tris-HCl, and 150 mM NaCl) in the presence of 1X protease inhibitor mixture (Roche). Tissue homogenates were centrifuged at 18,000 rcf for 30 min. Protein concentration in supernatants was determined using the BCA protein assay kit (Thermo Fisher Scientific). Equal amount of total proteins were run on 4–12% Bis-Tris XT gels (Bio-Rad Laboratories) and transferred to nitrocellulose membranes. Blots were probed with anti-apoE antibodies HJ6.1, HJ6.2, HJ6.3, or HJ6.4, as indicated in the figure. Equal amount of anti-apoE antibodies were used as a primary antibody to detect apoE in Western blotting. Blots were simultaneously exposed for the same period of time.

Immunoprecipitation. Protein G–Sepharose 4 Fast Flow beads (GE Healthcare) were washed with ice-cold PBS and resuspended in ice-cold PBS. The washed 50% beads were then mixed with each HJ6 series antibodies (0.4 µg/µl of 50% bead mixture) in the presence of 1% Triton X-100. Antibody beads were prepared by covalently binding HJ6 antibodies to protein G–Sepharose 4 Fast Flow beads. Freshly prepared dimethyl pimelimidate in 0.2 M triethanolamine (pH, 8.2; Sigma-Aldrich) was added to the beads to cross-link. The beads were then washed once with 50 mM Tris (pH, 7.5) to stop the cross-linking reaction. Brain cortex samples were lysed in 1% Triton X-100 lysis buffer (Triton X-100, 150 mM NaCl, 50 mM Tris-HCl, 1X complete protease tablet [Roche]). After centrifugation at 18,000 rcf for 30 min, the supernatant was collected and used for subsequent immunoprecipitation steps. The precleared lysates were then tumble incubated with HJ antibody-conjugated beads for immunoprecipitation.

Immunization of mice. 4-mo-old male APPswe/PS1ΔE9 mice (Jankowsky et al., 2004) were intraperitoneally injected weekly for 14 wk with PBS or anti-apoE antibody (HJ6.3) at 10 mg of antibody/kg of body weight dose. Working stock of antibody was freshly prepared on the date of injection at 1 mg/ml concentration. Brain tissues were collected 10 d after the last injection. For a short-term experiment, nine-month-old male APPswe/PS1ΔE9 mice were intraperitoneally injected 4 times every 3 d, and brain tissues were collected 24 h after the last injection. All animal experiments were approved by the animal study committee at Washington University in St. Louis.

Measurement of HJ6.3 antibody levels in cerebral cortex and plasma. 4-mo-old APPswe/PS1ΔE9 mice were intraperitoneally injected one time with biotinylated anti-apoE antibody (HJ6.3) at 10 mg of antibody/kg of body weight dose. After perfusion, cerebral cortical tissues were collected 24 h after injection, and then sonicated with PBS (100 mg of wet weight/ml of PBS). PBS lysates and plasma samples were loaded to anti–mouse IgG antibody-coated plate (10 µg/ml; Jackson ImmunoResearch Laboratories), and biotinylated HJ6.3 antibody was detected with poly-horseradish peroxidase streptavidin (Thermo Fisher Scientific) and Super Slow 3,3′,5,5′-tetramethylbenzidine (Sigma-Aldrich).

Histology and quantitative analysis of Aβ plaques. Brain hemispheres were placed in 30% sucrose before freezing and cutting on a freezing sliding microtome. Serial coronal sections at 50-µm intervals were collected from the rostral anterior commissure to caudal hippocampus. Sections were stained with biotinylated 82E1 (anti-Aβ1-16) antibody (1:500 dilution; IBL International) or X-34 dye. Stained brain sections were scanned with a NanoZoomer slide scanner (Hamamatsu Photonics) at 20× magnification setting. For quantitative analyses of 82E1-biotin and X-34 staining, scanned images were exported using NDP viewer software (Hamamatsu Photonics) and converted to 8-bit grayscale using ACDSee Pro 2 software (ACD Systems). All converted images were uniformly thresholded to highlight plaques, and then analyzed by "Analyze Particles" function in the ImageJ software (National Institutes of Health). Identified objects after thresholding were individually inspected to confirm the object as a plaque or not. 3 brain sections per mouse, each separated by 300 µm, were used for quantification. These sections correspond approximately to sections at Bregma −1.7, −2.0, and −2.3 mm in the mouse brain atlas. The mean of three sections was used to represent a plaque load for each mouse. For analysis of Aβ plaque in the cortex, the cortex immediately dorsal to the hippocampus was assessed. All analyses were performed in a blinded manner.

Quantitative analysis of CD45 staining. Brain sections cut with a freezing sliding microtome were immunostained with anti-CD45 antibody (1:500 dilution; AbD Serotec). Stained brain sections were scanned with a NanoZoomer slide scanner (Hamamatsu Photonics) at 40× magnification setting. The percent area covered by CD45 staining was analyzed in the cortex by using NDP viewer, ACDSee Pro 2, and ImageJ softwares, as described in the previous section. Three brain sections per mouse, each separated by 300 µm, were used for quantification. The mean of three sections was used to estimate the area covered by immunoreactivity. All analyses were performed in a blinded fashion after stained images were thresholded to minimize false-positive signals.

Measurement of IFN-γ and IL-1α. 9-mo-old male APPswe/PS1ΔE9 mice were intraperitoneally injected 4 times every 3 d, and brain tissues were collected 24 h after the last injection. Cerebral cortical tissues were lysed by sonication (3-s pulse, 5 times, 35% amplitude) with lysis buffer (50 mM Tris-HCL, 2 mM EDTA, 1 µg/ml leupeptin, 1 µg/ml aprotinin, 0.25 mM phenylmethanesulfonyl fluoride, pH 7.4). Homogenates were centrifuged for 10 min at 14,000 RPM. Supernatants were used to measure IFN-γ and IL-1α levels using Rodent Cytokine Multi-Analyte Profile (Myriad RBM).

Aβ and apoE ELISA. Cortical and hippocampal tissues were sequentially homogenized with PBS and 5 M guanidine buffer in the presence of 1X protease inhibitor mixture (Roche). The levels of insoluble Aβ in a 5-M guanidine fraction were measured by sandwich ELISA. For Aβ ELISA, HJ2 (anti–Aβ35-40) and HJ7.4 (anti–Aβ37-42) were used as capture antibodies, and HJ5.1-biotin (anti–Aβ13-28) was used as the detection antibody. ApoE levels in the plasma and cortical tissue PBS lysates were measured using apoE ELISA. HJ6.2 and HJ6.3 antibodies were used for capture and detection, respectively. Pooled C57BL/6J plasma was used as a standard for murine apoE quantification (Kim et al., 2009b).

Total cholesterol assay. 10 µl of plasma from each mouse was mixed with 1 ml of Color Reagent (Wako Chemicals USA), containing 1.6 U/ml cholesterol ester hydrolase, 0.31 U/ml cholesterol oxidase, 5.2 U/ml peroxidase, 0.19 mmol/l 4-aminoantipyrine, 4.4 U/ml ascorbate oxidase, and 0.95 mmol/l 3,5-dimethoxy-N-ethyl-N-(2-hydroxy-3-sulfopropyl) aniline sodium. After 5 min incubation at 37°C, absorbances of samples and standards were measured at 600 nm. Total cholesterol levels were calculated based on the standard curve.

Statistical analyses. To determine the statistical significance (*, $P < 0.05$; **, $P < 0.01$; ***, $P < 0.001$), two-tailed Student's *t* test was used (GraphPad Prism 5.0), after testing the equal variance test (Levene median test) and

normality test (Kolmogorov-Smirnov test; SigmaStat 3.0.). Variability of the measurements was reported as SEM.

We thank Robert Mach (Washington University) for providing the X-34 dye.

This work was supported by National Institutes of Health grants AG13956 (D.M. Holtzman), the Cure Alzheimer's Fund (D.M. Holtzman), Neuroscience Blueprint Center Core Grant P30-NS057105 (D.M. Holtzman), and P30NS069329 (J. Kim).

Washington University has filed a patent application for the use of anti-apoE antibodies as a treatment for AD. The authors of this manuscript are listed as inventors on that patent application. The authors have no further conflicts of interest.

Submitted: 14 June 2012
Accepted: 10 October 2012

REFERENCES

Bard, F., C. Cannon, R. Barbour, R.L. Burke, D. Games, H. Grajeda, T. Guido, K. Hu, J. Huang, K. Johnson-Wood, et al. 2000. Peripherally administered antibodies against amyloid beta-peptide enter the central nervous system and reduce pathology in a mouse model of Alzheimer disease. *Nat. Med.* 6:916–919. http://dx.doi.org/10.1038/78682

Bien-Ly, N., A.K. Gillespie, D. Walker, S.Y. Yoon, and Y. Huang. 2012. Reducing human apolipoprotein E levels attenuates age-dependent Aβ accumulation in mutant human amyloid precursor protein transgenic mice. *J. Neurosci.* 32:4803–4811. http://dx.doi.org/10.1523/JNEUROSCI.0033-12.2012

Brody, D.L., and D.M. Holtzman. 2008. Active and passive immunotherapy for neurodegenerative disorders. *Annu. Rev. Neurosci.* 31:175–193. http://dx.doi.org/10.1146/annurev.neuro.31.060407.125529

Castano, E.M., F. Prelli, T. Wisniewski, A. Golabek, R.A. Kumar, C. Soto, and B. Frangione. 1995. Fibrillogenesis in Alzheimer's disease of amyloid beta peptides and apolipoprotein E. *Biochem. J.* 306:599–604.

Castellano, J.M., J. Kim, F.R. Stewart, H. Jiang, R.B. DeMattos, B.W. Patterson, A.M. Fagan, J.C. Morris, K.G. Mawuenyega, C. Cruchaga, et al. 2011. Human apoE isoforms differentially regulate brain amyloid-β peptide clearance. *Sci. Transl. Med.* 3:89ra57. http://dx.doi.org/10.1126/scitranslmed.3002156

Deane, R., A. Sagare, K. Hamm, M. Parisi, S. Lane, M.B. Finn, D.M. Holtzman, and B.V. Zlokovic. 2008. apoE isoform-specific disruption of amyloid beta peptide clearance from mouse brain. *J. Clin. Invest.* 118:4002–4013. http://dx.doi.org/10.1172/JCI36663

DeMattos, R.B., J.R. Cirrito, M. Parsadanian, P.C. May, M.A. O'Dell, J.W. Taylor, J.A. Harmony, B.J. Aronow, K.R. Bales, S.M. Paul, and D.M. Holtzman. 2004. ApoE and clusterin cooperatively suppress Abeta levels and deposition: evidence that ApoE regulates extracellular Abeta metabolism in vivo. *Neuron.* 41:193–202. http://dx.doi.org/10.1016/S0896-6273(03)00850-X

Golde, T.E., P. Das, and Y. Levites. 2009. Quantitative and mechanistic studies of Abeta immunotherapy. *CNS Neurol. Disord. Drug Targets.* 8:31–49. http://dx.doi.org/10.2174/187152709787601830

Golde, T.E., L.S. Schneider, and E.H. Koo. 2011. Anti-aβ therapeutics in Alzheimer's disease: the need for a paradigm shift. *Neuron.* 69:203–213. http://dx.doi.org/10.1016/j.neuron.2011.01.002

Holtzman, D.M., J.C. Morris, and A.M. Goate. 2011. Alzheimer's disease: the challenge of the second century. *Sci. Transl. Med.* 3:sr1.

Jankowsky, J.L., D.J. Fadale, J. Anderson, G.M. Xu, V. Gonzales, N.A. Jenkins, N.G. Copeland, M.K. Lee, L.H. Younkin, S.L. Wagner, et al. 2004. Mutant presenilins specifically elevate the levels of the 42 residue beta-amyloid peptide in vivo: evidence for augmentation of a 42-specific gamma secretase. *Hum. Mol. Genet.* 13:159–170. http://dx.doi.org/10.1093/hmg/ddh019

Jiang, Q., C.Y. Lee, S. Mandrekar, B. Wilkinson, P. Cramer, N. Zelcer, K. Mann, B. Lamb, T.M. Willson, J.L. Collins, et al. 2008. ApoE promotes the proteolytic degradation of Abeta. *Neuron.* 58:681–693. http://dx.doi.org/10.1016/j.neuron.2008.04.010

Kim, J., J.M. Basak, and D.M. Holtzman. 2009a. The role of apolipoprotein E in Alzheimer's disease. *Neuron.* 63:287–303. http://dx.doi.org/10.1016/j.neuron.2009.06.026

Kim, J., J.M. Castellano, H. Jiang, J.M. Basak, M. Parsadanian, V. Pham, S.M. Mason, S.M. Paul, and D.M. Holtzman. 2009b. Overexpression of low-density lipoprotein receptor in the brain markedly inhibits amyloid deposition and increases extracellular A beta clearance. *Neuron.* 64:632–644. http://dx.doi.org/10.1016/j.neuron.2009.11.013

Kim, J., H. Jiang, S. Park, A.E. Eltorai, F.R. Stewart, H. Yoon, J.M. Basak, M.B. Finn, and D.M. Holtzman. 2011. Haploinsufficiency of human APOE reduces amyloid deposition in a mouse model of amyloid-β amyloidosis. *J. Neurosci.* 31:18007–18012. http://dx.doi.org/10.1523/JNEUROSCI.3773-11.2011

Koenigsknecht-Talboo, J., M. Meyer-Luehmann, M. Parsadanian, M. Garcia-Alloza, M.B. Finn, B.T. Hyman, B.J. Bacskai, and D.M. Holtzman. 2008. Rapid microglial response around amyloid pathology after systemic anti-Abeta antibody administration in PDAPP mice. *J. Neurosci.* 28:14156–14164. http://dx.doi.org/10.1523/JNEUROSCI.4147-08.2008

Lucin, K.M., and T. Wyss-Coray. 2009. Immune activation in brain aging and neurodegeneration: too much or too little? *Neuron.* 64:110–122. http://dx.doi.org/10.1016/j.neuron.2009.08.039

Ma, J., A. Yee, H.B. Brewer Jr., S. Das, and H. Potter. 1994. Amyloid-associated proteins alpha 1-antichymotrypsin and apolipoprotein E promote assembly of Alzheimer beta-protein into filaments. *Nature.* 372:92–94. http://dx.doi.org/10.1038/372092a0

Namba, Y., M. Tomonaga, H. Kawasaki, E. Otomo, and K. Ikeda. 1991. Apolipoprotein E immunoreactivity in cerebral amyloid deposits and neurofibrillary tangles in Alzheimer's disease and kuru plaque amyloid in Creutzfeldt-Jakob disease. *Brain Res.* 541:163–166. http://dx.doi.org/10.1016/0006-8993(91)91092-F

Sadowski, M.J., J. Pankiewicz, H. Scholtzova, P.D. Mehta, F. Prelli, D. Quartermain, and T. Wisniewski. 2006. Blocking the apolipoprotein E/amyloid-beta interaction as a potential therapeutic approach for Alzheimer's disease. *Proc. Natl. Acad. Sci. USA.* 103:18787–18792. http://dx.doi.org/10.1073/pnas.0604011103

Santuccione, A.C., M. Merlini, A. Shetty, C. Tackenberg, J. Bali, M.T. Ferretti, J. McAfoose, L. Kulic, C. Bernreuther, T. Welt, et al. 2012. Active vaccination with ankyrin G reduces β-amyloid pathology in APP transgenic mice. *Mol. Psychiatry.*

Wang, A., P. Das, R.C. Switzer III, T.E. Golde, and J.L. Jankowsky. 2011. Robust amyloid clearance in a mouse model of Alzheimer's disease provides novel insights into the mechanism of amyloid-β immunotherapy. *J. Neurosci.* 31:4124–4136. http://dx.doi.org/10.1523/JNEUROSCI.5077-10.2011

Wilcock, D.M., S.K. Munireddy, A. Rosenthal, K.E. Ugen, M.N. Gordon, and D. Morgan. 2004. Microglial activation facilitates Abeta plaque removal following intracranial anti-Abeta antibody administration. *Neurobiol. Dis.* 15:11–20. http://dx.doi.org/10.1016/j.nbd.2003.09.015

Wisniewski, T., and B. Frangione. 1992. Apolipoprotein E: a pathological chaperone protein in patients with cerebral and systemic amyloid. *Neurosci. Lett.* 135:235–238. http://dx.doi.org/10.1016/0304-3940(92)90444-C

Wisniewski, T., E.M. Castaño, A. Golabek, T. Vogel, and B. Frangione. 1994. Acceleration of Alzheimer's fibril formation by apolipoprotein E in vitro. *Am. J. Pathol.* 145:1030–1035.